The Thesis Committee for Erica Janette Powell
Certifies that this is the approved version of the following thesis:

Varying Flux Controls on Timescales of Autogenic Storage and Release Processes in Fluvio-deltaic Environments: Tank Experiments

APPROVED BY
SUPERVISING COMMITTEE:

Supervisor:

Wonsuck Kim

Ronald Steel

David Mohrig

Varying Flux Controls on Timescales of Autogenic Storage and Release Processes in Fluvio-deltaic Environments: Tank Experiments

by

Erica Janette Powell, B.S.Geo.Sci.

Thesis

Presented to the Faculty of the Graduate School of

The University of Texas at Austin

in Partial Fulfillment

of the Requirements

for the Degree of

Master of Science in Geological Sciences

The University of Texas at Austin

May 2011

Acknowledgements

This study was supported by a Jackson School of Geosciences at the University of Texas at Austin research grant and a postdoctoral fellowship in Japan Society for the Promotion of Science (JSPS) to W.K. This work has also been partially supported by the William R. Muehlberger Field Geology Scholarship fund. We would like to thank Professor Tetsuji Muto at Nagasaki University, Japan for allowing us access to his laboratory facilities, considerable help during the experiments, and also for stimulating discussion.

Abstract

Varying Flux Controls on Timescales of Autogenic Storage and Release Processes in Fluvio-deltaic Environments: Tank Experiments

Erica Janette Powell, M.S.Geo.Sci.

The University of Texas at Austin, 2011

Supervisor: Wonsuck Kim

Changes in external forcing having traditionally been the main area of interest in trying to understand paleo-depositional environments in sedimentary systems; however, autogenic variability has been rising in importance, while autogenic behavior has been thought of as a "noise" generator. Recently, autogenic variability has been rising in attention because decoupling allogenic signatures (externally driven) from the stratigraphic record requires robust understanding of autogenic variations (internally generated). This study aims to quantitatively measure autogenic processes under a range of flux conditions and to show that autogenic processes generate distinct signatures rather than random noise. We present data from a matrix of nine different tank experiments in order to systematically evaluate the effects of sediment flux and water discharge variations on the autogenic timescale of fluvial sediment storage and release processes and the implications of this data to the stratigraphic record. The sediment flux tow ater discharge ratio and the absolute values of these two discharges control the autogenic

timescale. Variations in sediment supply yield two competing effects on the autogenic timescale. The primary sediment flux control causes a reduction in the autogenic timescale as an increase in sediment supply yields an increased rate of filling the "fluvial envelope" (the space between the maximum and minimum fluvial slopes obtained during storage and release events). In contrast, the secondary sediment flux control increases the size of the fluvial envelope and works against the primary sediment flux control. Increasing the water discharge increases the autogenic timescale by widening the fluvial envelope during the organization of the fluvial system and more importantly, diminishes the functionality of the secondary sediment control. A competition exists between these factors, causing a non-linear range of autogenic timescales for a given sediment flux to water discharge ratio. In the nine experiments here, as the ratio decreases, the secondary effects of variations in sediment supply are suppressed by the relatively high water discharge, and the timescale is more predictable using the primary sediment control. As the ratio increases, the secondary effects from sediment supply are enhanced by a poorly organized fluvial system, and the timescale converges to a narrow range. This suggests significant implications for autogenic sediment delivery and stratigraphic development in a wide range of discharge conditions in field cases.

Table of Contents

List of Tables

List of Figures

Introduction

Sedimentary processes and their resulting stratigraphic architecture they create provide crucial clues to paleo-depositional environments. The rock record consists of sedimentary patterns that were developed due to changes in allogenic conditions as well as patterns that were developed autogenically (i.e. delta lobe/channel avulsion, sediment storage and release). *Muto et al.* [2007] delineates the term 'autogenic' as intrinsic responses to steady external forcing and 'allogenic' as responses to non-steady external forcing. Traditionally, changes in shoreline migration and stratigraphic sequences have been attributed to unsteady changes in external dynamic factors (i.e. global sea-level changes, tectonic subsidence/uplift, and sediment supply changes) [*Galloway*,1989a; *Galloway*, 1989b; *Helland-Hansen & Gjelberg*, 1994; *Helland-Hansen & Martinsen*, 1996; *Posamentier & Vail*, 1988; *Posamentier et al.*, 1988; *Vail et al*., 1977; *Van Wagoner et al*., 1988; *Watts*, 1982]. Decoupling these allogenic signatures (externally driven) from autogenic variations (internally generated), is key to correctly deciphering paleo-environmental variations in the sedimentary record. Autogenic products in the sedimentary record have generally been thought of as minor "noise" and are not understood well enough to quantify autogenic signatures [*Kim & Jerolmack*, 2008]. However, recent studies have shown that internally generated responses can be cyclic in nature, and they play an important role in the sedimentary record [*Ashworth et al*., 2004; *Bryant et al.*, 1995; *Cazanacli et al.*, 2002; *Heller et al.*, 2007; *Hickson et al.*, 2005; *Jerolmack &* Mohrig, 2005; *Kim &* Jerolmack, 2008; *Kim &* Muto, 2007; *Kim & Paola,* 2007; *Kim et al.*, 2006a; *Mohrig et al.*, 2000*; Muto & Steel*, 2001; *Muto & Steel*, 2004; *Paola*, 2000; *Paola et al.*, 2001; *Paola et al.*, 2009; *Sheets et al.*, 2002]. Non-steady external forcing (variation in the rate of base-level rise or variation in sediment supply) is

important as traditionally viewed; however, autogenic responses during both steady and non-steady external conditions should also be considered. In the present study, internal responses during steady external forcing are analyzed. Quantitative understanding of autogenic processes and their stratigraphic deposits will offer a more fundamental understanding of the stratigraphic record, as this facilitates the separation of stratigraphic data into allogenic and autogenic products.

Experimental stratigraphy [*Paola et al.*, 2001] and flume/tank experiments provide a useful tool for understanding large-scale stratigraphic and morphodynamic responses and also for beginning to understand how to separate allogenic and autogenic signatures in the rock record [*Gerber et al.*, 2008; *Heller et al.*, 2001; *Hickson et al.*, 2005; *Kim et al.*, 2006b; *Kim & Paola*, 2007; *Kim et al., 2010; Kostic et al.,* 2002; *Martin et al.*, 2009; *Muto*, 2001; *Muto & Steel*, 2001; *Muto & Steel*, 2004; *Muto & Swenson*, 2006; *Reitz et al.*, 2010; *Van Dijk et al.*, 2009]. Recent studies using tank experiments have demonstrated distinct shoreline position fluctuations due to autogenic fluvial sediment storage and release [*Kim & Jerolmack*, 2008; *Reitz et al.*, 2010; *Van Dijk et al.*, 2009]. *Ashmore* [1991] has suggested a similar process of internally generated pulses due to aggradation and degradation in braided, gravel-bed streams. These experiments have shown that under constant sediment supply and upstream water discharge settings, flow on the topset of deltas alternates between discrete periods of sheet flow and channelized flow. Here, sheet flow is used in the sense of *Hogg* [1982] in which flow is relatively high-frequency, low magnitude overland flow as continuous sheets experiencing laminar flow conditions. This alternation causes fluctuations in the shoreline migration rate over time with an overall progradational trend in the experimental deltas. These fluctuations occur at regular intervals and they are caused by the cyclic nature of fluvial-mass storage (sheet flow) and release (channelization). During times of sheet flow, the flow widens

and becomes laterally unconfined, which enhances deposition on the topset surface of the delta. Because most of the sediments are being stored on the topset surface, sediments are not being fed into the basin which causes a slowly prograding, or stationary, shoreline. This alluvial aggradation steepens the overall slope of the delta topset until a critical threshold slope value is reached. At this time, the system is no longer able to sustain the maximum slope and incision inevitably begins to occur so that the topset slope is reduced [*Parker et al.*, 1998]. The position where a convex-up fluvial profile (upstream) meets a concave-up fluvial profile (downstream) is where the slope is maximized, and channel initiation occurs at this inflection point, migrating upstream as a knickpoint [*Kim & Jerolmack*, 2008]. A period of strong channelization begins to release sediments into the basin due to an increase in transport capability. An increased amount of sediment is transported during enhanced channelization due to the nonlinearity of sediment transport relations [*Parker et al.*, 1998]. This produces a great increase in the rate of the shoreline progradation. Eventually, cutting of the deltaic topset due to channelization, which is more focused upstream, reduces the overall topset slope of the delta to a point where backfilling of the channel begins to occur. Sheet flow deposition resumes again once the channel is filled with supplied sediment. Alternations between sheet flow and channelized flow produces cyclic fluctuations in the shoreline progradation rate and the topset slope through time. The alluvial slope of the deltaic topset is an important control in this process and has been shown to be inversely related to water discharge, secondarily related to sediment flux [*Whipple et al.*, 1998], and linearly correlated to the sediment flux to water discharge ratio [*Parker et al.*, 1998].

While these studies have shown quantitative data illustrating this cyclic process of sediment storage and release, there are some missing experiments to fully understand the autogenic processes. This study aims to fill in some of these gaps. The experimental

studies from *Kim & Jerolmack* [2008] used two different experiments for their study that kept the sediment flux (Q_s) to water discharge (Q_w) ratios constant ($Q_s/Q_w \approx .01$) which causes similar overall deltaic surface slopes; however, different absolute values of sediment and water were used. *Van Dijk et al.* [2009] ran three different experiments with constant Q_s, but varied the Q_w to explore how changes in water discharge affected this process. Experiments that evaluate changes in Q_s while keeping Q_w constant have not yet been undertaken. This study aims to analyze these missing experiments as well as to add to the existing knowledge on the subject. Here, a matrix of nine different experiments allows for systematic analysis of solely the effects of changes in Q_s, Q_w, and Q_s/Q_w on the autogenic storage and release processes. Quantitative measurements of the storage and release process are obtained from the changes in the shoreline migration rate. A numerical model is also used to extract the autogenic variations from the overall shoreline progradational trend. The effects of the Q_s/Q_w ratio, Q_s, and Q_w on the autogenic timescale will be explored and correlated to morphological changes in the fluvio-deltaic system. This has implications for fluvial incision and terrace development as well as significance for source to sink sediment deposition and development of erosional surfaces.

Experiment

Experimental Setup

For this study, a matrix of nine different experiments was used to test the effects of Q_s, Q_w, and Q_s/Q_w on autogenic storage and release timescales (Figure 1). All of the experiments were conducted in a basin with dimensions of 1 m wide and 1 m long at Nagasaki University, Japan (Figure 2). Each experiment used a mixture of sediment and water that was delivered into the basin, building a delta over a flat, non-erodible basement into a standing body of water. The sediment mixture contained two different grain sizes and used 50% fine sand (D = 0.1 mm) and 50% coarse sand (D = 1 mm) by volume. The sediment was pre-mixed with water and fed into the basin as a point source, located in the corner of the experimental basin. Initial base level for these experiments was kept constant at 3 cm, measured from the basement, and no subsidence was applied. Keeping these external factors constant throughout each experimental run allow for analysis of only the autogenic variation. All factors were kept constant during each run, and the only changing elements between experiments were sediment flux and water discharge. A 1.2 cm thick gravel layer was placed over the basement floor before each experiment to ensure a flat, non-erodible surface. The total run time for the different experiments varied because different sediment flux values filled up the basin at different rates (Table 1), but each delta was built to about 80-90 cm away from the sediment and water point source. This allowed multiple autogenic cycles to be obtained, which ranged between 4-8 cycles. The experimental parameters are shown in Table 1. The sediment flux values ranged from 0.5 cm^3/s (low Q_s runs) to 2 cm^3/s (high Q_s runs). For the water discharge, 65 cm^3/s was used for the high discharge runs and 16.25 cm^3/s was used for the low discharge runs. This yielded Q_s/Q_w values that range from 0.015 at the lowest, to 0.246 at the highest. The individual experiments will be referred to by acronyms that

pertain to the sediment and water input parameters for the particular experiment. For instance, the experiment at the bottom right hand corner of the design matrix (Figure 1) has a high value for water discharge (65 cm^3/s) and a high value for sediment flux (2 cm^3/s). This experiment will be referred to as HwHs because of the high water value and high sediment value. A low water discharge run (16.25 cm^3/s) with a medium sediment flux (1 cm^3/s) will be referred to as LwMs, a medium water discharge run (32.5 cm^3/s) with a low sediment flux (0.5 cm^3/s) will consequently be referred to as MwLs, and so on.

Table 1: Experimental Parameters

Experiment	Q_s/Q_w	Q_s (cm^3//s)	Q_w (cm^3/s)	Average Slope (S_t)	Run Time (hrs)
HwLs	0.015	0.5	65.0	0.043	6.18
HwMs	0.03	1.0	65.0	0.058	4.30
HwHs	0.06	2.0	65.0	0.077	2.50
MwHs	0.123	2.0	32.5	0.103	3.00
MwMs	0.06	1.0	32.5	0.077	1.16
MwLs	0.03	0.5	32.5	0.058	7.0
LwLs	0.06	0.5	16.2	0.077	7.0
LwMs	0.123	1.0	16.2	0.103	5.0
LwHs	0.246	2.0	16.2	0.136	3.0

METHODS AND DATASET

In order to capture the deltaic evolution, high resolution time-lapse photos were taken every 20 seconds for each experiment from two different locations (overhead and side, Figure 2). The water was dyed a blue color in order to increase visibility. The blueness in the photos was first converted to grayscale, and then to black and white images using a certain threshold value. This threshold value is a water depth proxy which allowed for the experimental deltaic surface to be starkly contrasted with the standing water (ocean), outlining the shoreline for each image (Figures 3A and 3B). The shoreline

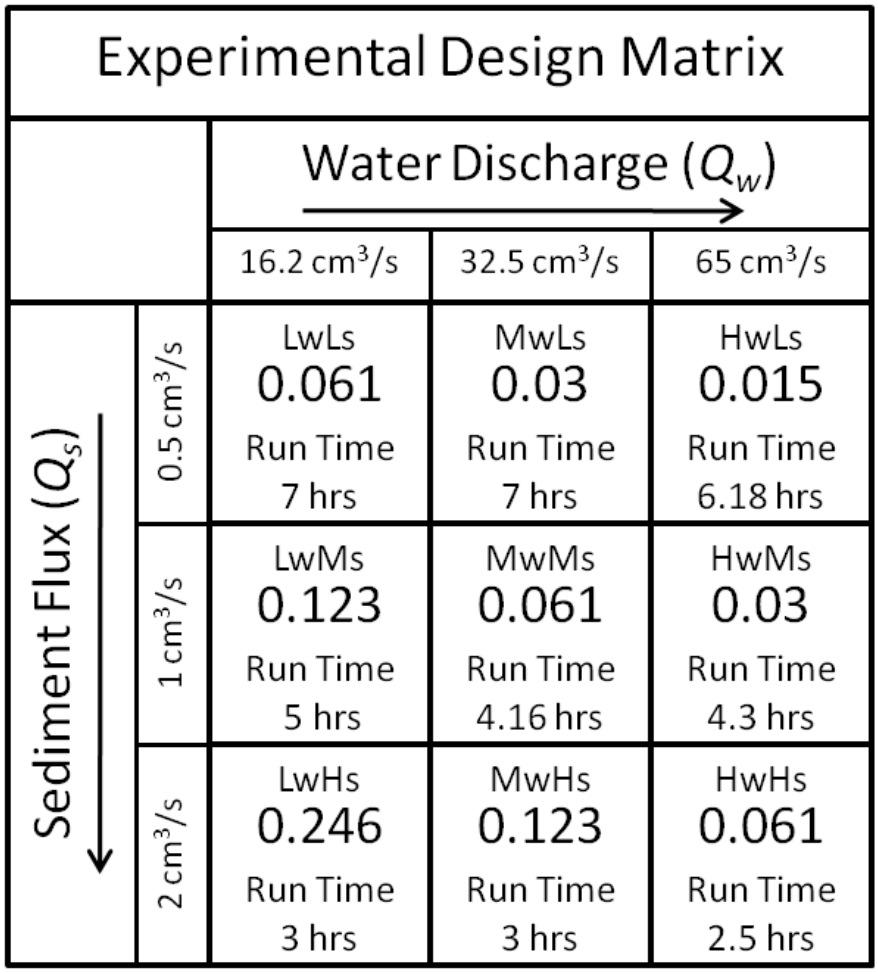

Figure 1: Matrix depicting the experimental design and Q_s/Q_w ratios. Three values of Q_w and three values of Q_s were used to yield 9 different experiments with different parameters. The experiment identifiers are shown in the upper portion of the box. The overall Q_s/Q_w ratios are shown in the center, and the experimental run time is shown in the bottom of each box.

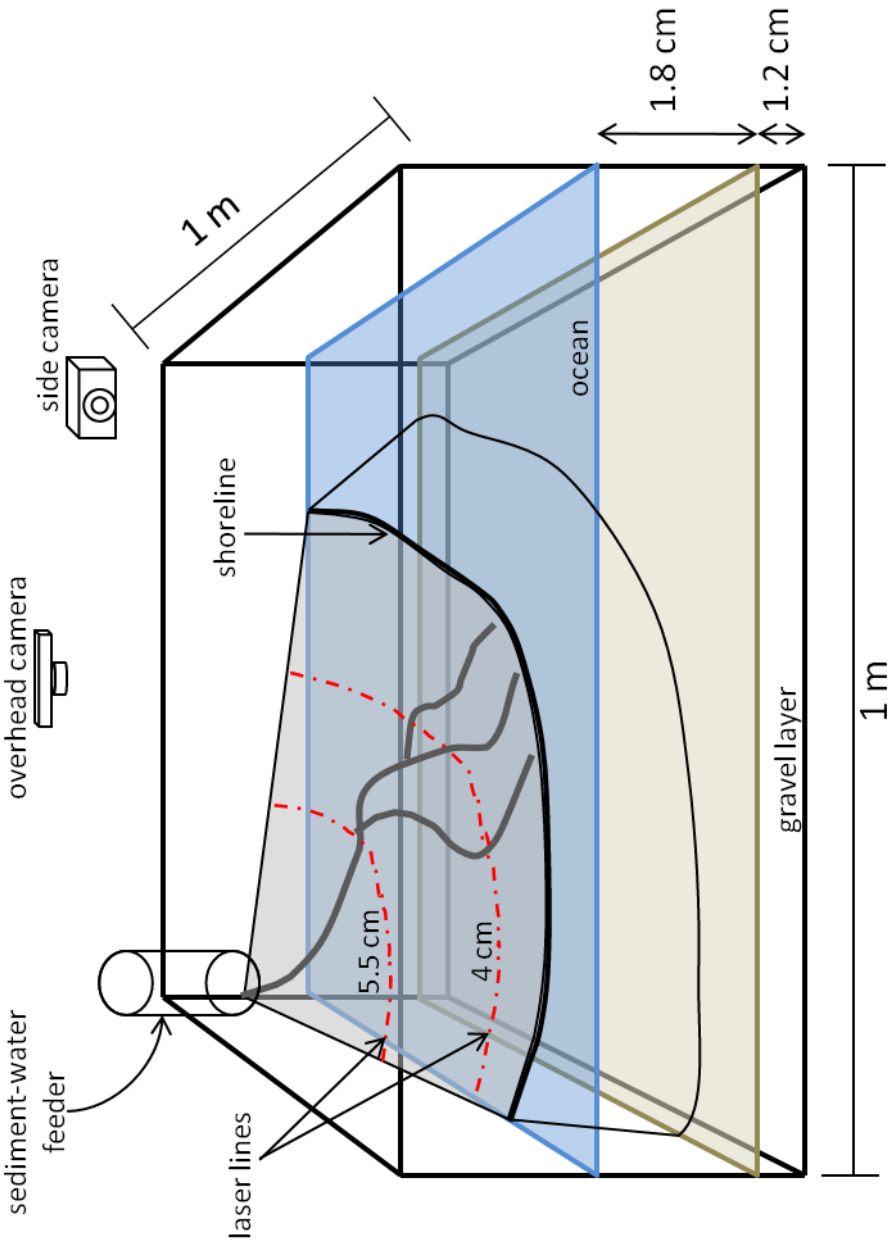

Figure 2: Schematic diagram of the experimental setup and basin dimensions.

was mapped automatically using each of the black and white images (Figures 3C and 3D). A laterally averaged shoreline position was extracted from the overall mapped shoreline by using the average length of each shoreline point away from the point source location for each image. This produced an average shoreline position through time for each experiment.

Laser lines were projected onto the deltaic surface at different heights (4 cm and 5.5 cm from the basement floor). These laser lines acted as topographic lines of equal elevation that were used to measure the slope of the topset surface of the experimental delta. Three known elevations (the water surface at 3 cm, a laser line at 4 cm, and a second laser at 5.5 cm) allowed for detailed slope measurements over the topset of the delta. For every 15 images (i.e., every 5 minutes of experimental run time), the slopes were measured along three different transects on the top o the deltaic surface when the delta had built to a sufficient size. Three different slope measurements were collected along each transect. This ensured more accurate values for the topset slope (S_t) both through time and overall for each experiment. The slope of the foreset (S_f) was also measured, but showed much less variability than the topset slope. This slope was measured using the known water surface elevation and the known basement elevation along the three different transects; however, due to the more consistent nature of this measurement, the slopes were measured every 50 images.

EXPERIMENTAL RESULTS

Each of the 9 experiments shows a purely progradational shoreline migration trend (Figure 4). Because base level remained stationary, the system also remained purely aggradational [*Muto et al.*, 2007]. Figure 4 indicates that autogenic events are superimposed over the long-term progradational trend. A small-scale increase in the rate

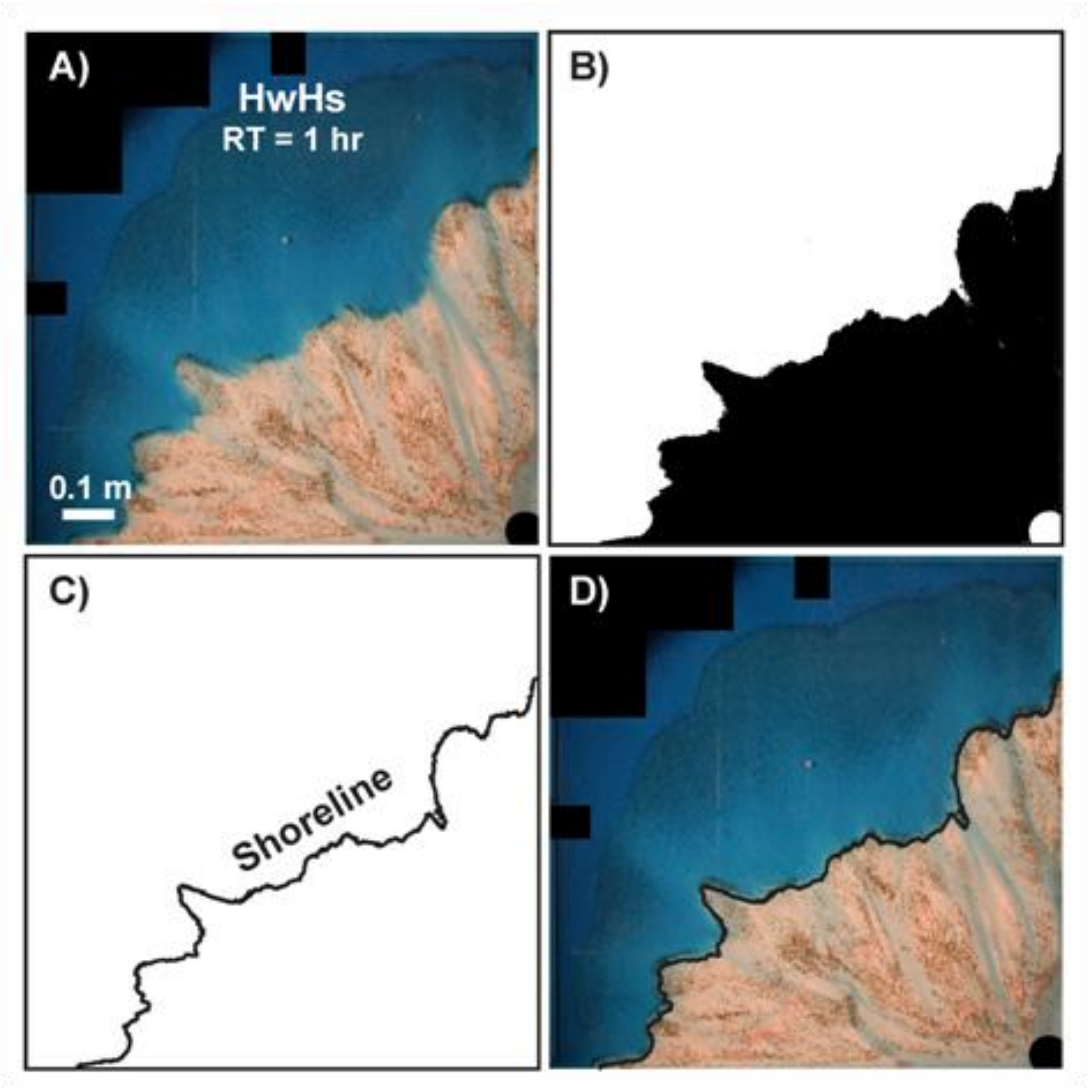

Figure 3: A) Overhead image taken from experiment HwHs at run time (RT) 1 hour, prior to any manipulation, B) image as a result of automatic color manipulation. The deltaic surface is black and the ocean is white showing a clearly defined boundary, C) resulting mapped shoreline, and D) original image overlain by the automatically extracted shoreline.

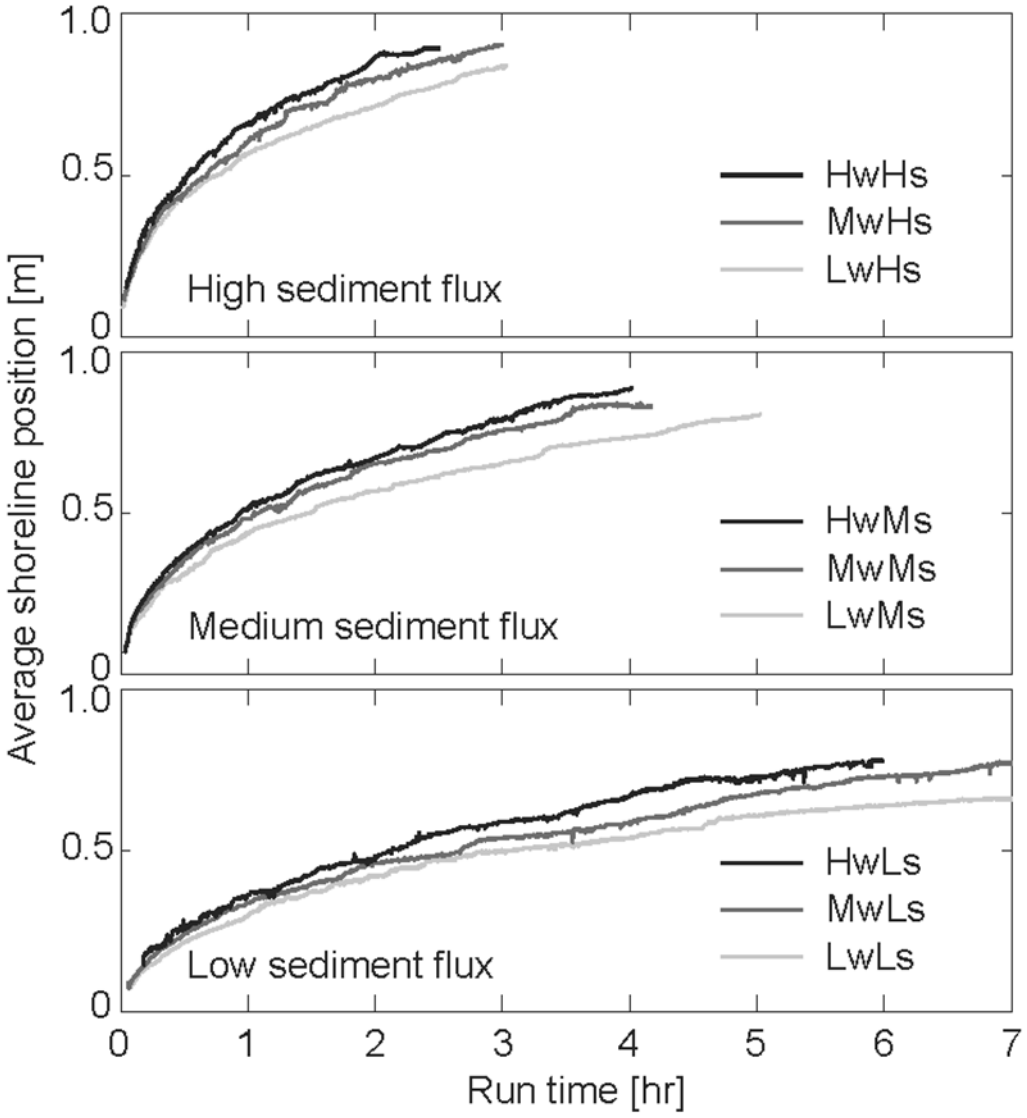

Figure 4: All 9 experiments grouped by experimental runs that have constant sediment flux values. High sediment flux, medium sediment flux, and low sediment flux, from top to bottom.

of shoreline progradation compared to the general migration trend indicates a time of autogenic release due to strong channelization. However, when this curve shows a slower, or stagnate, rate of progradation, a period of storage is dominant [*Kim & Jerolmack*, 2008]. Due to different overall values of sediment flux and water discharge, the rate of progradation is similar among experiments with the same sediment flux, even though different amounts of water discharge change the topset slope and lead to slightly different overall shoreline migration trends. The importance of sediment flux versus water discharge in the autogenic storage and release timescales will be discussed in more detail.

Changes in the map-view patterns of the shoreline geometry can be seen in the experimental time-lapse images. Both highly rough shoreline and quite smooth shoreline geometries can be seen in the images and can also be linked to the Q_s/Q_w ratio (Figures 5A and 5B). Figures 5A and 5B show an example of different shoreline geometries observed in HwLs and LwLs respectively, ranging from quite rough (with delta lobe development), to more smooth and symmetrical. More stable channels are seen in concert with the low Q_s/Q_w ratios, which allows for strong delta lobe development and a rough shoreline in planform. However, as the Q_s/Q_w ratio increases, the shoreline roughness decreases, or the shoreline becomes much smoother as seen in Figure 5B.

The slope range for each experiment was calculated using the maximum and minimum 10^{th} percentiles of slope measurements. This range is indicative of how much space exists between the highest level of aggradation (highest slope) and the lowest level of sediment release by channelization (lowest slope). The slope range can also be described as a buffer, as defined by *Holbrook et al.*, [2006], in which the term buffer was

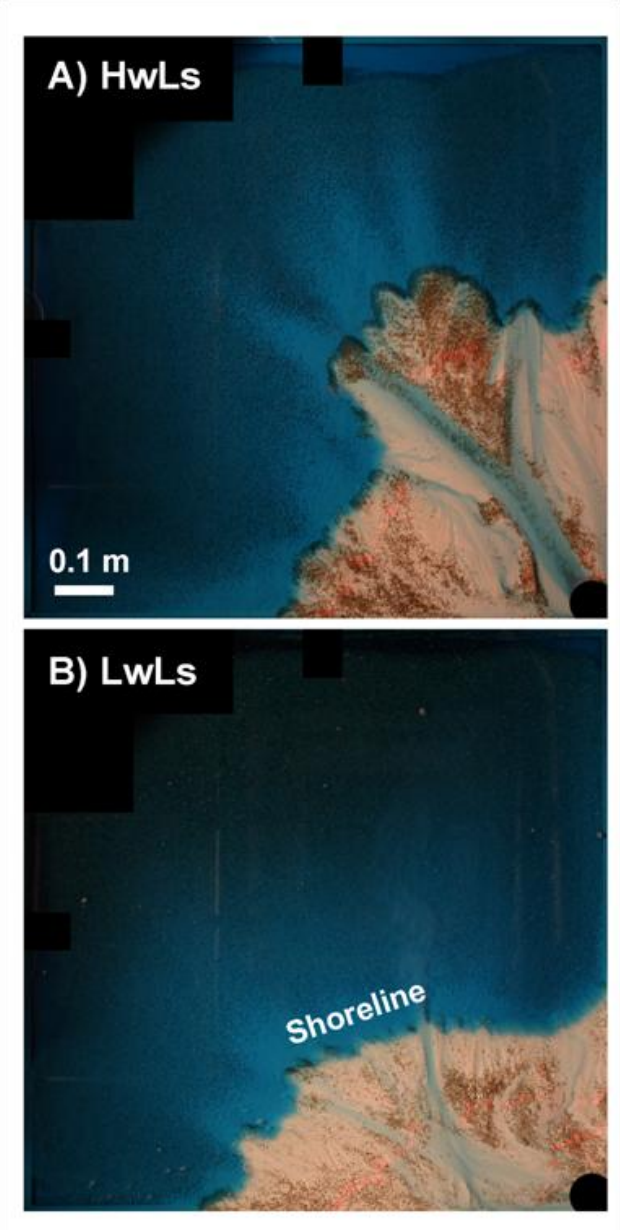

Figure 5: A) Photo taken from experiment HwLs (RT, 2.3 hr) during a release event, with a low Q_s/Q_w ratio, showing a rough shoreline with delta lobe protrusion and a deep, straight channel. B) Photo taken from experiment LwLs (RT, 3 hr) during a release event, with a high Q_s/Q_w ratio, showing a smoother shoreline, with no significant lobe formation and a highly disorganized channel system.

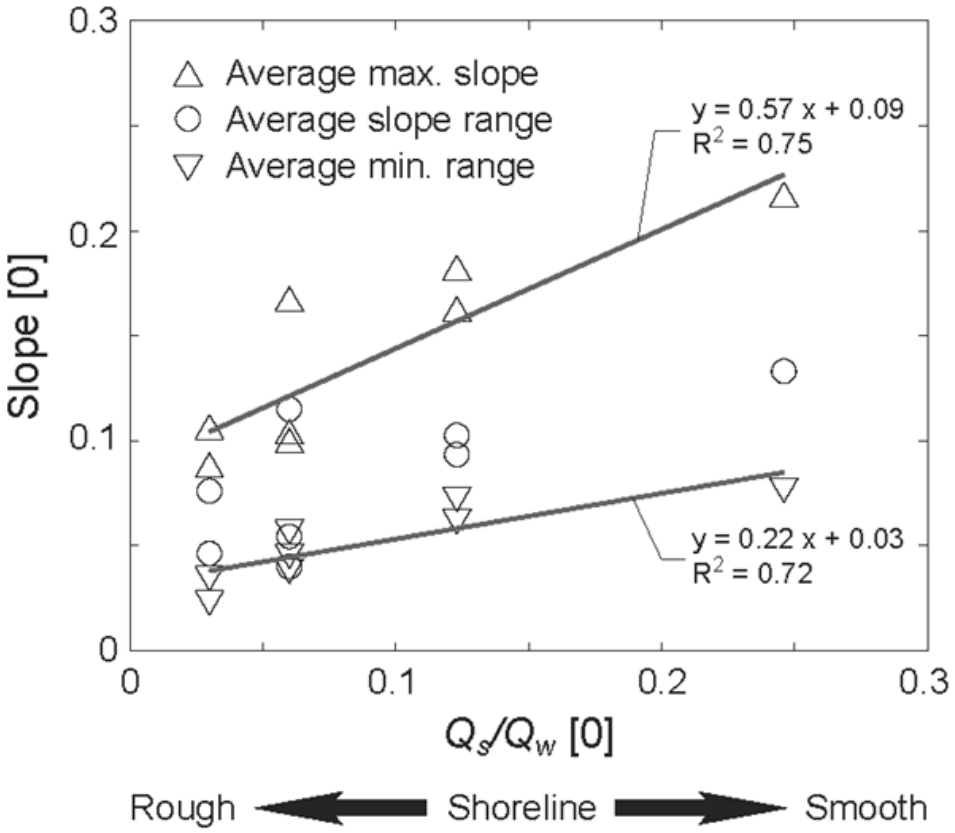

Figure 6: Average minimum slope, maximum slope and slope range associated with each Q_s/Q_w ratio. Plot shows a general increase in the slope range (circles) with an increasing Q_s/Q_w ratio. A shoreline with no roughness would be a perfectly symmetrical shoreline and a rough shoreline would have defined protrusions from lobe formation

proposed to describe conceptual surfaces: 1. the potential maximum aggradational surface and 2. the potential maximum level of incision in a longitudinal river profile. While the application of the term "buffer" in this study does not meet the definition of *Holbrook et al.* [2006] exactly, a similar conceptualization can be utilized with the two dynamic fluvial profiles that occur during sediment storage and release [*Kim et al.*, 2006]. The space between these two buffers encases the available fluvial preservation space, and here it is shown that the magnitude of this space changes with changing Q_s/Q_w ratios. The relationship between the magnitude of the slope ranges and the Q_s/Q_w ratio is shown in Figure 6. A positive relationship exists between these two factors, indicating that the space created during a storage and release cycle, increases with increasing Q_s/Q_w ratio. However, the rate at which the created space (the "envelope") is filled is not linearly related to Q_s. This will be explored further. In any case, the low Q_s/Q_w runs, or the runs with a small slope range, show the roughest shoreline geometries, while runs with large slope ranges, show smoother shoreline geometries.

Geometric Shoreline Model

NUMERICAL MODEL DERIVATION

A simple geometric model was developed in order to mathematically model the shoreline position through time to accompany the experimental data. This model aims to capture the general progradational trend and not the autogenic variation of the shoreline as a moving boundary [*Swenson et al.*, 2000]. The definition sketch for the numerical model parameters can be seen in Figure 7A. The delta deposit can be characterized into two different geometries: a cylinder and a cone (Figure 7B). The cylinder shape approximates the bottom deposit, while the cone shape approximates the top deposit assuming a linear surface slope. Simplified geometric models similar to that presented here, have been applied to model deltaic evolution in scaled experiments and field studies [*Kim et al.*, 2006; *Heller et al.*, 1993; *Petter & Muto*, 2008]. A mass-balance of supplied sediments balancing with 1) the volume of the top of the delta by using ¼ the volume of a cone, and 2) the volume of the bottom of the delta by using ¼ the volume of a cylinder can be represented with the following form:

(1)

where s denotes the shoreline position, u denote the delta toe position, Z denotes the base level height, H denotes the height from base level to the most upstream point, Q_s denotes the sediment flux at the point source, and t denotes time. However, some parameters in this governing equation are unknowns (H and u). The slope components from the definition sketch can be used to substitute unknown variables for known or measured parameters to calculate the downstream shoreline position. The slope components here are:

(2a)

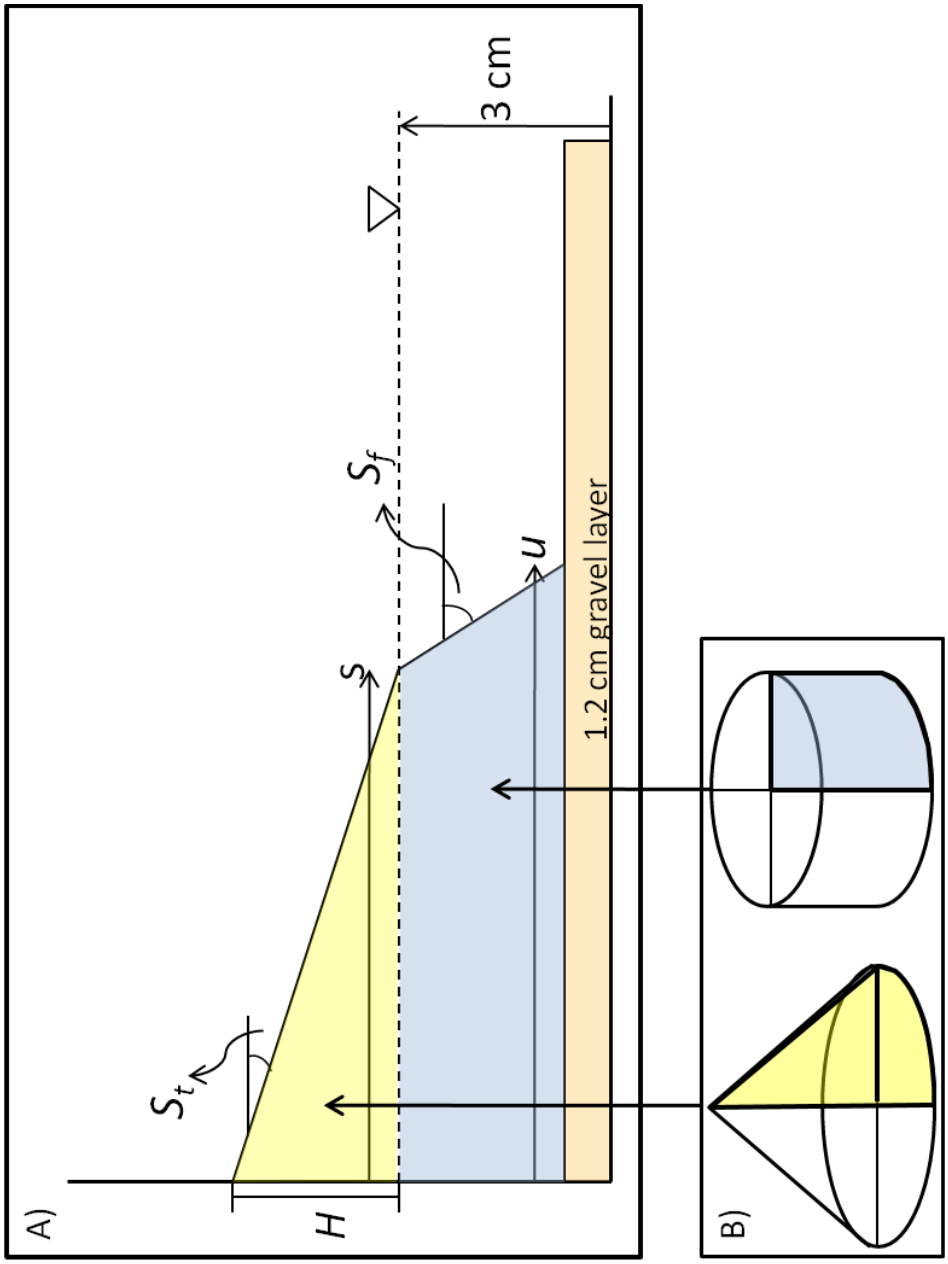

Figure 7: A) Definition sketch for numerical model parameters and B) geometric bodies used to approximate the total volume of the delta.

(2b)

where S_t denotes the average linear topset slope, and S_f denotes the average foreset slope. Substituting relationship derived from (2a) and (2b) into the governing equation (1) yields:

(4)

Solving for s will yield an equation for the position of the shoreline through time with known input and measured parameters. The cubic formula is used to find an equation for s in terms of these variables. The cubic formula involves defining coefficients for the third order polynomial above (4) to solve for the wanted variable s:

(4)

where:

(5a)

(5b)

(5c)

Here it is assumed that Q_s, Z, S_f, and S_t are constant with time and thus p, α, and β are constant. The above formulation is algebraically complex; however, it is important to understand that the shoreline position (s) is modeled as a function of the cube root of time ($t^{1/3}$) in a radially growing delta.

NUMERICAL MODELING RESULTS

The experimental parameters (Table 1) were applied to the numerical model derived above to capture the overall progradational trend of the experimental delta. As shown in the numerical derivation, the shoreline position through time is a function of Q_s, Z, S_f, and S_t. Most significantly, the topset slope (S_t) is one of the most important

variables in modeling the shoreline migration, and this value is controlled by the ratio of sediment flux (Q_s) to water discharge (Q_w). As the ratio increases, the average topset slope value increases. Figure 8A shows an example of the numerical model compared with the actual shoreline position measured from the experiments. The numerical model shows an overall progradational trend while the experimental model shows progradation along with autogenic fluctuations in the shoreline through time. This is significant because the model does not depict autogenic variability, but instead, it is a simplified geometric model that shows large-scale trends. Deviations from the overall trend are caused by autogenic storage and release events. In order to extract the autogenic fluctuations through time, the model results were used to de-trend the long-term shoreline migration component by differencing the two curves (Figure 8B). Therefore, the result is solely the fluctuations due to autogenic storage and release events represented by troughs and peaks respectively.

This model captures the shoreline migration using the cube root of time relationship instead of the square root of time that is often used in modeling two-dimensional deltaic evolution [*Reitz et al.*, 2010; *Kim et al.*, 2006; *Swenson et al.*, 2000]. Both relationships indicate that with external forcing held constant, deltas will initially prograde quickly, but the progradation rate non-linearly decreases through time. Due to the three-dimensional nature of these experiments, it is important to capture the cube root function because this causes the shoreline migration rate to decrease faster than it would with a model using the square root of time.

NORMALIZATION

The shoreline position and experimental run time data were both normalized in order to create non-dimensional numbers that could be analyzed free from constrains of

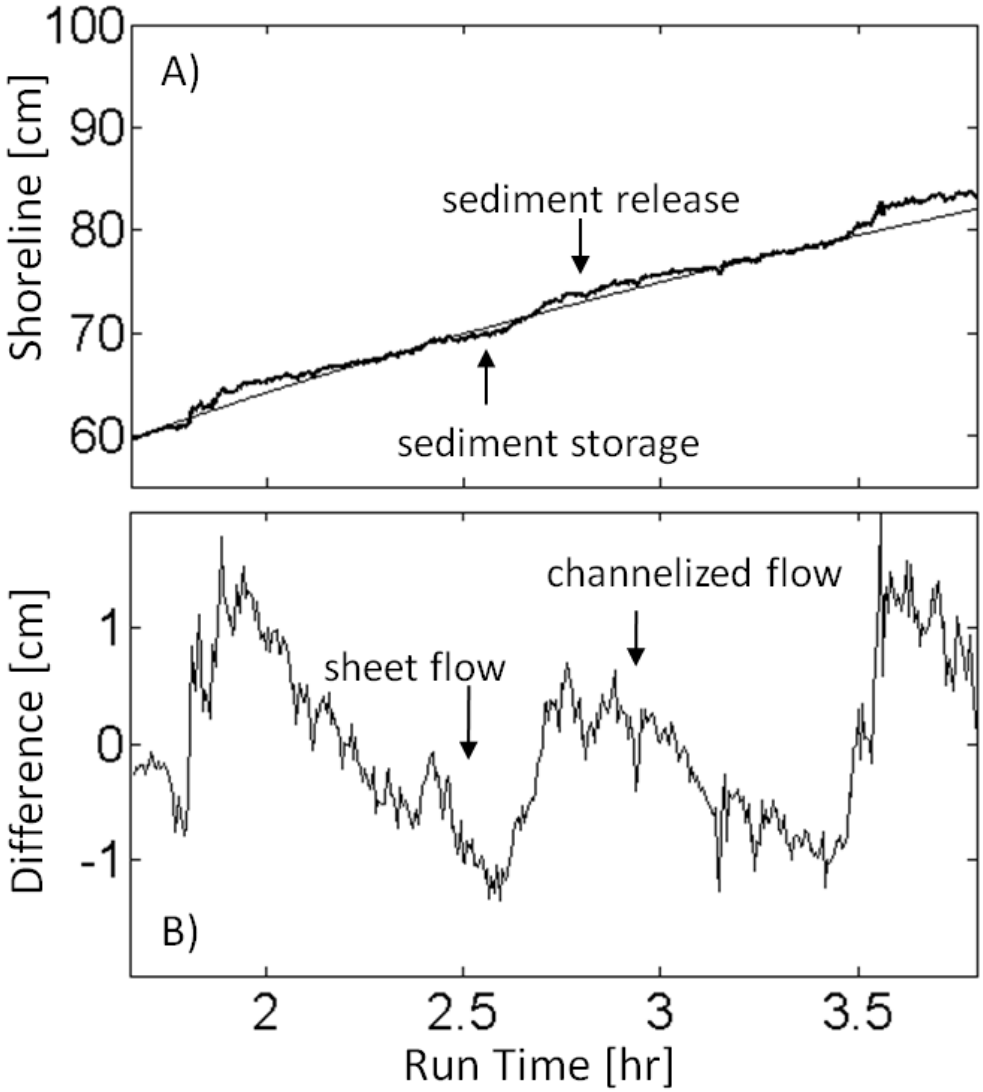

Figure 8: A) From experiment MwMs, (1.6 to 3.8 hrs), the experimental average shoreline position in the thick black line and the numerically modeled shoreline position in the thin black line. B) The difference between the numerical model shoreline and the experimental average shoreline with time. Fluctuations represent storage and release events. Peaks represent release events (when the average shoreline is greater than the numerically modeled shoreline) and troughs represent storage (when the average shoreline position is less than the numerically modeled shoreline).

scale for individual experiments, using a characteristic length scale (L) and timescale (T_{DC}) respectively.

$$-\qquad (6a)$$

$$—\qquad (6b)$$

where L is the characteristic backwater length, and h is the channel depth. The average channel depth was estimated to be 1 cm, while the average topset slope (S_t) was calculated from the average of the measured slopes over all nine experiments. This is the same approach as presented in *Postma et al*. [2008], in which the equilibrium timescale is described by a characteristic volume representing the system and the characteristic transport rate (Q_s).

Autogenic Timescales

As mentioned above, the de-trended shoreline time series data was used to quantitatively measure the autogenic fluctuations. Figure 8B shows the time series curve that represents deviations of the shoreline location from the overall trend derived from the numerical model, indicating that either dominant release or storage was occurring. Statistical methods and time series analysis were used in order to detect the number of peaks (release events) from the curve in concert with spectral plots showing different orders of frequencies in the data (Figures 9A and 9B, respectively). The first method used a certain window length to re-sample the time series data and extract the most significant trends. The main cycle frequency reflecting storage and release processes can then be manually picked for each experiment by using the number of release events that occur per hour of experimental run time (Figure 9A). Secondly, the spectral plot method shows different orders of cycle frequencies derived from a Fourier transformation (Figure 9B). This method automatically detected multiple hierarchy-order frequencies from the curve that results from autogenic processes. The most significant, or first-order frequency signal, is shown as the largest peak, and this was used to detect the autogenic frequency generated for each experimental run. These two methods were used in concert with each other to ensure accurate frequency and timescale measurements for storage and release processes. The autogenic timescale can then be defined by the reciprocal of the frequency data which gives an approximate time period between release events. The frequency and timescale data were normalized by the characteristic timescale for each experiment to take a dimensionless form.

Table 2 shows the autogenic frequencies/timescales associated with both real and normalized data for each experiment. For consistency, the autogenic timescale in this

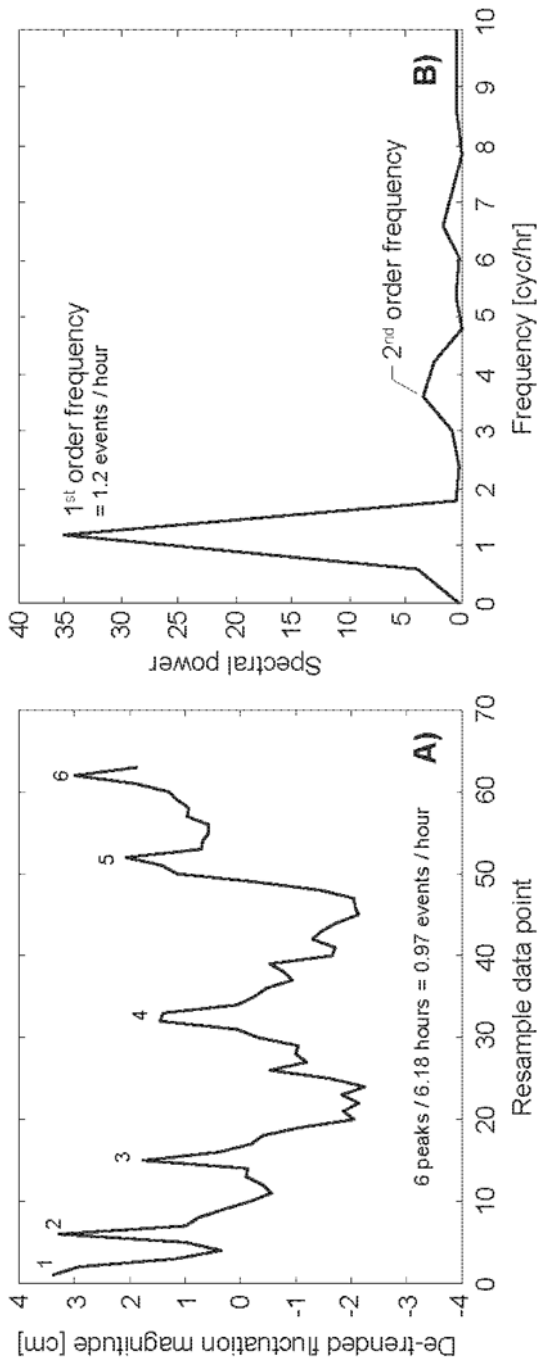

Figure 9: A) Example of the re-sampling technique from HwLs showing 6 peaks, or release events and B) Example of the spectral plot from experiment HwLs. The x-axis shows the cycle frequency and the y-axis shows the spectral plot of the extracted frequency. The most significant frequency is the result of the autogenic storage and release sequence.

study was calculated for only the portion of the experimental run time until the shared maximum basin characteristic time among the nine experiments. While the timescale increased with run time for individual experiments, to gain the correct trend of timescale variation between experiments, it was important to use the data over a consistent duration across the experiments.

Table 2: Autogenic Frequency and Timescale Results

	Real		Normalized	
Experiment	Frequency (cyc/hr)	Timescale (hr)	Frequency	Timescale
HwLs	1.2	0.833	0.053	18.779
HwMs	1.69	0.592	0.049	20.137
HwHs	2.02	0.495	0.039	25.273
MwHs	2.0	0.500	0.052	19.210
MwMs	1.65	0.606	0.065	15.470
MwLs	1.4	0.714	0.082	12.154
LwLs	1.71	0.585	0.133	7.464
LwMs	2.0	0.500	0.104	9.605
LwHs	2.4	0.417	0.083	12.088

Experimental results (Table 2) show that as sediment flux increases (Q_s/Q_w increases), the autogenic frequency also increases, while the autogenic timescale decreases (Figure 10A). This is evident for each of the three groups of experiments that have a constant water discharge and increasing sediment flux. The groups of experiments with constant sediment flux, but varying water discharge values, show that as water discharge decreases (Q_s/Q_w increases), the frequency of autogenic storage and release also slightly increases (i.e., the timescale decreases) (Figure 10B). In general, the autogenic frequency increases as Q_s/Q_w increases; however, it is also observed that experiments with the same Q_s/Q_w ratio do not always show similar autogenic timescales (Figure 11A). This indicates that there are other factors affecting the autogenic timescale. Autogenic storage and release must depend on the absolute value of Q_s and Q_w, and their

ratio. The trend of the normalized data for the autogenic timescale and frequency are slightly different than the calculated data, and this will be discussed in more detail.

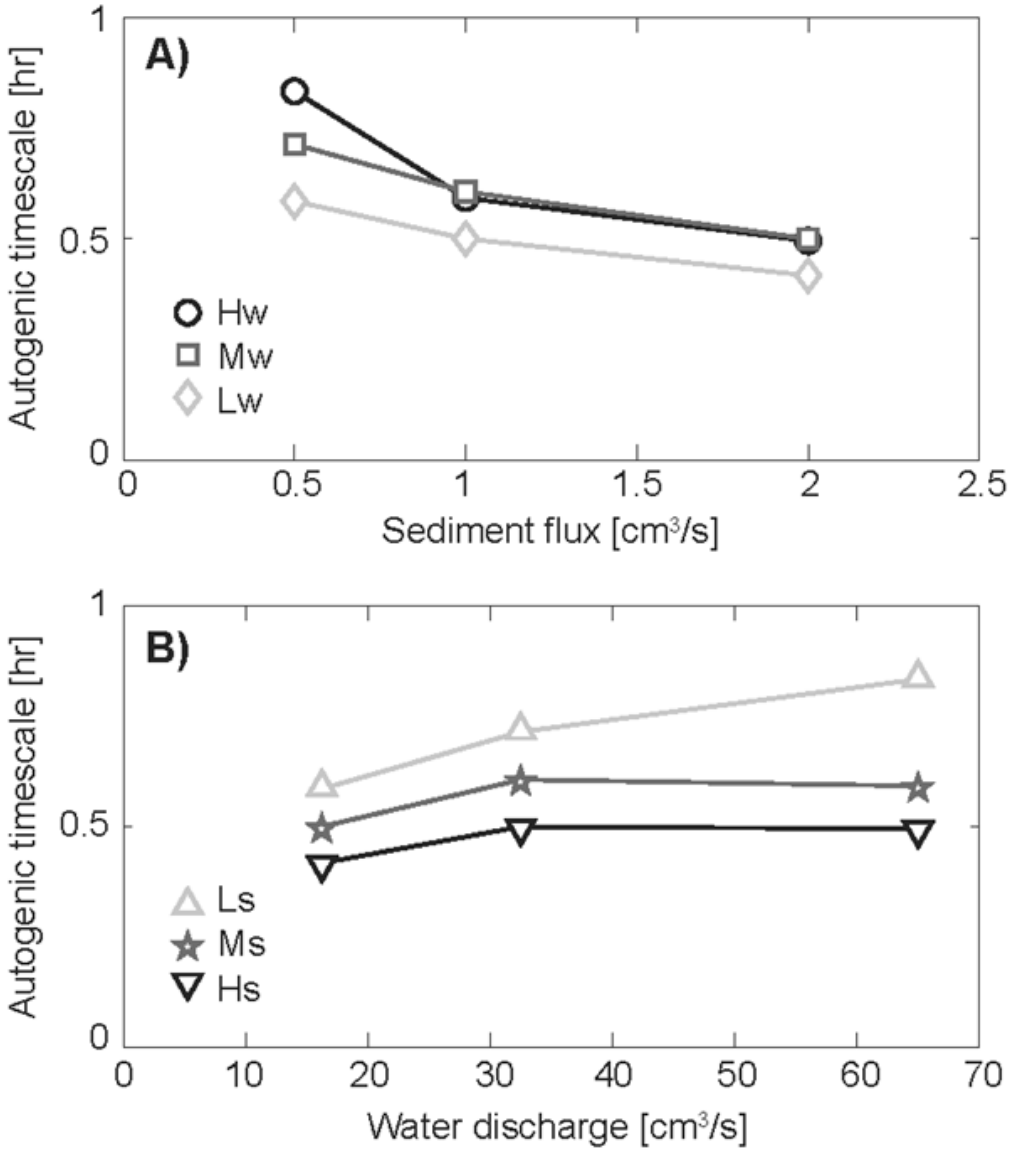

Figure 10: A) Plot showing sediment flux (cm^3/s) versus the autogenic timescale (hr) grouped by experiments with constant water discharge. As sediment flux increases (Q_s/Q_w increases), the timescale decreases. B) Plot showing water discharge (cm^3/s) versus the autogenic timescale (hr) grouped by experiments with constant sediment flux. As water discharge increases, the timescale increases as a general trend.

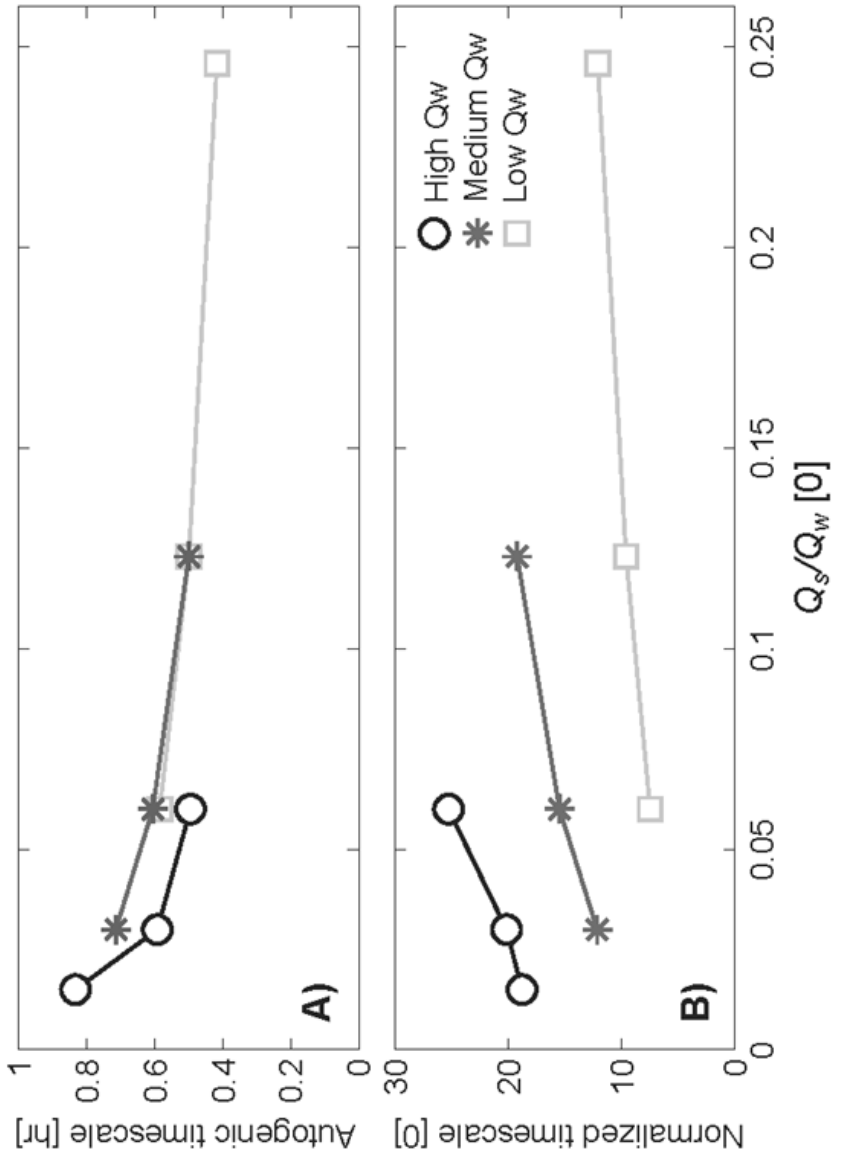

Figure 11: Plots showing the relationship between increasing sediment flux (increasing Q_s/Q_w) and the autogenic timescale grouped by constant water discharge runs. A) As the sediment supply increases, and Q_s/Q_w increases, the autogenic timescale decreases due to increasing sediment supply. B) As sediment supply increases and Q_s/Q_w increases, the normalized autogenic timescale increases indicating the increase in the size of the fluvial envelope.

Interpretation and Discussion

ROLE OF SEDIMENT FLUX IN AUTOGENIC TIMESCALES

A change in sediment flux is an important control in fluvio-deltaic environments. It has been shown that an increases in sediment supply can: 1) be a powerful driver for deltaic progradation even during times of base-level rise or highstand conditions [*Carvajal & Steel*, 2006], 2) increase channel mobility and confluence formation [*Ashmore*, 1991], and 3) be a factor in channel avulsion to an increase in location deposition [*Martin et al.*, 2009; *Mohrig et al.*, 2000]. Here, changes in sediment flux affect the frequency of autogenic storage and release events, or the small pulses of change in the shoreline migration rate on an overall shoreline trajectory (purely progradational in this study). The frequency of the fluvial autogenic processes is closely related to the avulsion and/or delta lobe switching frequency, but here the analysis uses the laterally averaged shoreline of which three-dimensional effects are eliminated. The fluvial autogenic processes in this study encompass the fluvial activity such as lateral channel migration, avulsion, and lobe switching as a whole.

As sediment flux increases, the recurrence of autogenic release events increases. More sediment is available to fill the space created during release events and to increase the deltaic topset slope to a maximum critical value. Therefore, the increased sediment supply shortens the time over which the fluvial envelope is filled and decreases the autogenic timescale (Figure 10A). This is consistent with the sediment flux control on the avulsion period estimated in *Reitz et al.* [2010]. They estimated the avulsion timescale is inversely proportional to the sediment discharge and is proportional to the channel volume (the channel-cross sectional area times the fluvial length). However, as mentioned above, the envelope size (the fluvial buffer: space between the maximum and minimum topset slopes) is not equal for each Q_s/Q_w ratio, but instead, it increases as the

Q_s/Q_w ratio increases (Figure 6). Using the difference between the average minimum and maximum topset slope values, the fluvial envelope (or buffer) acting over the autogenic storage and release events can be estimated. The slope range of the fluvial envelope, $\Delta S = 0.35(Q_s/Q_w) + 0.055$, increases with the Q_s/Q_w ratio. For example, MwHs has a high Q_s/Q_w ratio of 0.123 and MwLs has a Q_s/Q_w ratio of 0.03 (Table 1), and this difference is expected to force a 1.5 times increase in the slope range of the fluvial envelope. Only considering the sediment flux control, it might be expected that the autogenic frequency would linearly increase with an increase Q_s; however, when the fluvial buffer enlarges due to an increase in the Q_s/Q_w ratio, more time is necessary to fill a bigger envelope. Comparing MwHs and MwLs, it should be expected that a four times longer autogenic timescale would result from a four-fold decrease in the sediment supply rate; however, MwLs only shows an approximately 1.5 times longer autogenic timescale. Therefore, autogenic storage and release is less frequent than what would be expected with a linear relationship (Figure 10A). As shown in Figure 10A, the decreasing rate of the decrease in timescale with an increase in Q_s (i.e. the concave-up) reflects this effect.

Considering Table 2, the normalized autogenic timescales actually show the opposite trend that was calculated from the data, i.e., the timescale increases (frequency decreases) with increasing sediment flux. Recall that the equilibrium timescale from Equation (6b) was used to normalize the experimental data. The characteristic timescale is a function of sediment flux, average channel depth and average slope. Therefore, using this normalization, changes in the fluvio-deltaic system due to differences in the external conditions, e.g. different sediment supplies in different experiments, are minimized. The increase in the autogenic timescale shows the relative increase in the size of the fluvial envelope with increasing sediment flux. In other words, the longer timescale in the

normalized high sediment flux runs reflects a larger space to fill in the fluvial system with a given normalized sediment flux (Figure 11B).

In summary, a competition exists between the fluvial buffer and the available sediment supply to fill the space. Assuming a constant envelope size, increasing the amount of sediment flux would intuitively cause a proportionally shorter autogenic timescale. However, as the sediment supply is doubled, the frequency of release events is not doubled. This nonlinear relationship is caused by the modified envelope size associated with different sediment supply conditions.

ROLE OF WATER DISCHARGE ON AUTOGENIC TIMESCALE

Varying water discharge and holding sediment flux constant affects the autogenic event timescale as well. In general, as water discharge increases, the autogenic timescale increases (frequency decreases) (Figure 10B). In these cases, sediment flux is not changing for each set of three experiments, so the changes in Q_w are responsible for the increase in timescale. An important control in this aspect is the transport efficiency of the system, which decreases with a decrease in water discharge [*Bryant et al.*, 1995; *Whipple et al.*, 1998]. A decrease in the capacity for the system to transport sediment causes less sediment to be delivered into the basin and more sediment to fill the fluvial buffer space. This high net deposition on the fluvial surface is a factor in decreasing the autogenic timescale with a decrease in water discharge (Figure 10B). The amount of Q_w also affects the frequency by affecting the organization of the fluvial system (flow pattern). As Q_w decreases, a more organized, channelized system is less likely to develop during the release stages (Figure 5). For example, consider the first row in the design matrix (Figure 1), experiments LwLs, MwLs, and HwLs. The water discharge in HwLs was the maximum among these experiments (65 cm^3/s), and the fluvial system was highly

organized during release events (i.e. the channelization was pronounced, and the channel was deep and straight in geometry). However, in experiments MwLs and LwLs a successively decreasing amount of water discharge caused the channels to become much more braided and less stable in nature even during their sediment release stages. A lower water discharge caused a narrower range of the fluvial pattern change between the fully braided and channelized flows, and thus, shortened the time that it takes to switch between release and storage processes.

In summary, for experiments with decreasing water discharge, both the increases in net deposition and disorganization in the fluvial system contribute to the increase in autogenic frequency. The magnitude of release events also decreases with decreasing water discharge. Instead of long stable periods of progradation during release events (e.g., HwLs), the release events come in small, short pulses (e.g., LwLs) due to a change in the organizational nature of the fluvial system.

ROLE OF SEDIMENT FLUX TO WATER DISCHARGE RATIO

The sediment flux to water discharge ratio contributes to the roughness of the map-view shoreline geometry (i.e. strong local lobe progradation). A smoother shoreline is mainly caused by the frequent autogenic processes as the Q_s/Q_w ratio increases (Figure 5B). Frequent autogenic storage and release processes allow for sediment dispersal across the perimeter of the shoreline to be more uniform, resulting in smoother shoreline geometries. While there have been other studies that have shown shoreline roughness can be affected by other factors such as sediment mixtures and cohesiveness [*Martin et al.*, 2009], it is shown here that autogenic storage and release processes can also affect the shoreline roughness. This also indicates that the magnitude of release events with a

higher Q_s/Q_w ratio is smaller than the magnitude of release events with a lower Q_s/Q_w ratio for individual autogenic events.

The ratio of Q_s/Q_w is negatively correlated with the autogenic storage and release timescale (Figure 11A). However, experiments with the same Q_s/Q_w ratio did not result in strictly the same timescale values. This indicates that while there is a strong correlation between the Q_s and Q_w values and the autogenic timescale, the competition between the Q_s and Q_w controls is not a deterministic relationship with their ratio, but instead, non-linearly correlated with the individual Q_s and Q_w values. For instance, consider experiments HwHs, MwMs, and LwLs, which have the same Q_s/Q_w ratio, but different overall values of Q_s and Q_w. It has already been shown that the roles of sediment flux and water discharge play distinct roles in affecting the autogenic timescale by influencing the fluvial system itself. These controls lead to a negative correlation between the Q_s/Q_w ratio and the autogenic timescale, but there is a range of timescales that are applicable for a given Q_s/Q_w ratio.

While a range of timescales exists for a given Q_s/Q_w ratio, quantitatively, it is still unknown how to predict the extent of this range; however it can be shown that this range is not constant over all ratios. Figure 11A shows that the autogenic timescale curves, grouped by experiments with constant water discharge values, diverge with lower Q_s/Q_w ratio and converge with higher ratios. At higher Q_s/Q_w ratios, there is less variation in autogenic timescales, while at lower ratios, there is more variation in autogenic timescales. Differential effectiveness of the Q_s and Q_w controls on the fluvial evolution under different ratios accounts for this range. As shown here, sediment flux primarily affects the rate of filling of the fluvial envelope and secondarily influences the size of the envelope created during autogenic release events, while water discharge affects the overall organization of the fluvial system. These controls play against each other,

resulting in the autogenic frequency for given values of Q_s and Q_w. However, even if both of the Q_s and Q_w values change with the same rate, the effects of each Q_s and Q_w controls on the fluvial autogenic processes change with different rates under a given Q_s/Q_w ratio. For instance, from experiment HwMs to HwLs, the Q_s/Q_w ratio remains the same at 0.03, but there are two-fold decreases in both water discharge and sediment flux. HwMs shows the autogenic timescale of 0.592 hours while MwLs shows 0.714 hours (Table 2), and thus, about a 1.2 times increase in the autogenic timescale. However, the MwHs and LwMs experiments, both keeping the Q_s/Q_w ratio at 0.123 and the same two-fold change in water discharge and sediment flux, do not show (or very slightly show) an increase in the autogenic timescale (0.5 hours for both MwHs and LwMs). It would be expected to see the same two-fold decrease in the timescale for these two sets of experiments assuming linear variations in the response of the autogenic processes to the flux controls. Therefore, for a given ratio, there is a range of timescales that is ultimately controlled by the strongly coupled effect of the non-linearly varying Q_s and Q_w controls on the fluvial system.

Quantifying the differential effectiveness of the Q_s and Q_w controls under a given Q_s/Q_w ratio is beyond the scope of this paper. A qualitative assessment of this complex behavior is given here. Two end member cases to explain the behavior of sediment and water controls will be given. Sediment supply changes have a minimum impact at lower ratios (relatively small concentrations of sediment) on the buffer size modification, and thus the autogenic timescale follows changes in sediment supply more linearly. In contrast, at higher Q_s/Q_w ratios (high sediment concentration), the effects of sediment supply changes are maximized, and the primary sediment control (reduction in the autogenic timescale by an increased filling rate) is significantly dampened by the secondary sediment control (buffer size increase by a higher sediment flux). Lower Q_s/Q_w

ratios (relatively high water discharge) develop a highly organized fluvial system, and the system behaves more deterministically, while higher ratios (relatively lower water discharge) show a more stochastic behavior of the fluvial organization and thus suppresses the range of the autogenic timescales.

The timescale divergence is highlighted further when considering experiments from previous studies [*Kim & Jerolmack*, 2008]. Experiments from the Experimental Earthscape (XES) facility, XES 02 and XES 05, are reported on in *Kim & Jerolmack* [2008], *Kim et al.*, [2006a] and *Kim & Paola* [2007]. The XES 02 experiment used 5 times larger sediment and water discharges than XES 05, but the Q_s/Q_w ratios for both experiments were consistently kept at ~0.01, which is lower than the lowest ratio considered in this study. In XES 02, a 3-5 times shorter autogenic timescale was observed compared to that in XES 05 (i.e., approximately 2-3 hours for XES 02 and 8-10 hours for XES 05) [*Kim & Jerolmack,* 2008]. Considering the primary sediment flux control, a 5-fold increase in the sediment discharge could induce a 5-fold decrease in the autogenic timescale because of the higher sediment supply available to fill the fluvial envelope. The value that was observed from the two XES 02 and 05 experiments is close to this prediction. These two experiments show that even slightly lower Q_s/Q_w ratios have a much wider range of autogenic timescales, highlighting the divergence occurring at lower ratios due to the more organized system that reflects different sediment supply rates.

In the XES experiments, a different sediment mixture was used than the mixture presented in this study, which may have affected the range of the autogenic timescales for given Q_s/Q_w ratios as well. Two finer grain sizes in the XES sediment mixture produce a relatively smooth and symmetrical shoreline planform. The same XES experimental conditions with the mixture that was used in this study would yield a more organized channel pattern and thus, a rougher shoreline, which would widen the range of the

autogenic timescale for the ratio of 0.01. Other factors might be at play such as grain size distribution and proportions in sediment mixtures, which affect the autogenic timescale range. Nonetheless, there is a complicated relationship between the Q_s/Q_w ratio, sediment supply, and water discharge that ultimately yields different autogenic storage and release timescales.

IMPLICATIONS FOR STRATIGRAPHY AND FIELD CASES

Autogenic storage and release processes can be recognized in fluvial systems in the form of terrace formation. While changes in environmental conditions are important, autogenic incision is another mechanism for generating multiple terraces in fluvial environments [*Muto & Steel*, 2004]. In the experiments presented here, terrace development was observed, but temporary in nature due to stationary base level conditions. *Erkens et al*. [2009] explore terrace levels in the northern Upper Rhine Graben for the past 20 ky. They show five terrace levels that are different in terms of their elevations, morphologies, and sediment characteristics and argue for allogenic and autogenic controls on the formation of terrace levels. While older terrace levels formed during climatic warming triggered incision and a distinct change from a braided to meandering system, autogenic controls offer an alternate interpretation for younger Holocene terraces. *Erkens et al*. [2009] present this alternate idea that autogenic incision affected Holocene terraces in the Upper Rhine Graben. The Graben is a subsiding basin and environmental conditions during the Holocene were rather consistent so the younger terrace formation is best explained by autogenic controls, and it has been shown here that autogenic storage and release is a practical explanation for the terrace development. Autogenic periods of incision dominate the Holocene fluvial system in the Rhine Graben. Due to the subsiding tectonic conditions in the basin, incision would not be expected to

be active, but due to autogenic factors, three terrace levels have formed in these conditions. *Erkens et al.* [2009] interpret allogenic changes in climate to be the cause for terrace development during the Pleistocene; however, they argue for autogenic controls in terrace formation in the Holocene.

The understanding of autogenic storage and release processes is important for stratigraphic interpretation in terms of source to sink sediment deposition and development of erosional boundaries. Fluvial-dominated deltas at the shelf edge are efficient for delivering high volumes of sediment into deep-water slope and basin floor environments [*Carvajal & Steel*, 2009; *Edwards*, 1981; *Porebski & Steel*, 2003; *Berg*, 1982]. It is generally accepted that alterations in external forcing are the major control for variations in sediment delivering from deltas into deep water as basin floor fans and sediment supply for turbidites [*Carvajal & Steel*, 2009; *Kolla & Perlmutter*; 1993; *Johannessen & Steel*, 2005]. Consider two basins with a sandy deltaic system at or near the shelf edge feeding sediment into the basin. One has a Q_s/Q_w ratio comparable to HwLs and the other is comparable to LwLs. The storage and release process occurring on these two deltas would be quite different, and this would impact the deposits on the slope or in the basin. The HwLs delta would have longer duration and larger magnitude autogenic sediment delivery possibly causing turbidity flows and turbidite deposits in thick unified successions separated by periods of storage, or non-deposition on the slope/basin floor. In the case of the LwLs delta, sediment delivery would be short and minimal, but it would happen more frequently. This might cause autogenic sediment deposition to result in thin sandy layers from the delta overlain by thin layers of fine grained sediments that settle out from suspension. Figures 12A and 12B show a schematic model of how autogenic processes might affect the deposits in basin floor fans. Figure 12A shows a vertical section through a hypothetical basin floor fan with short

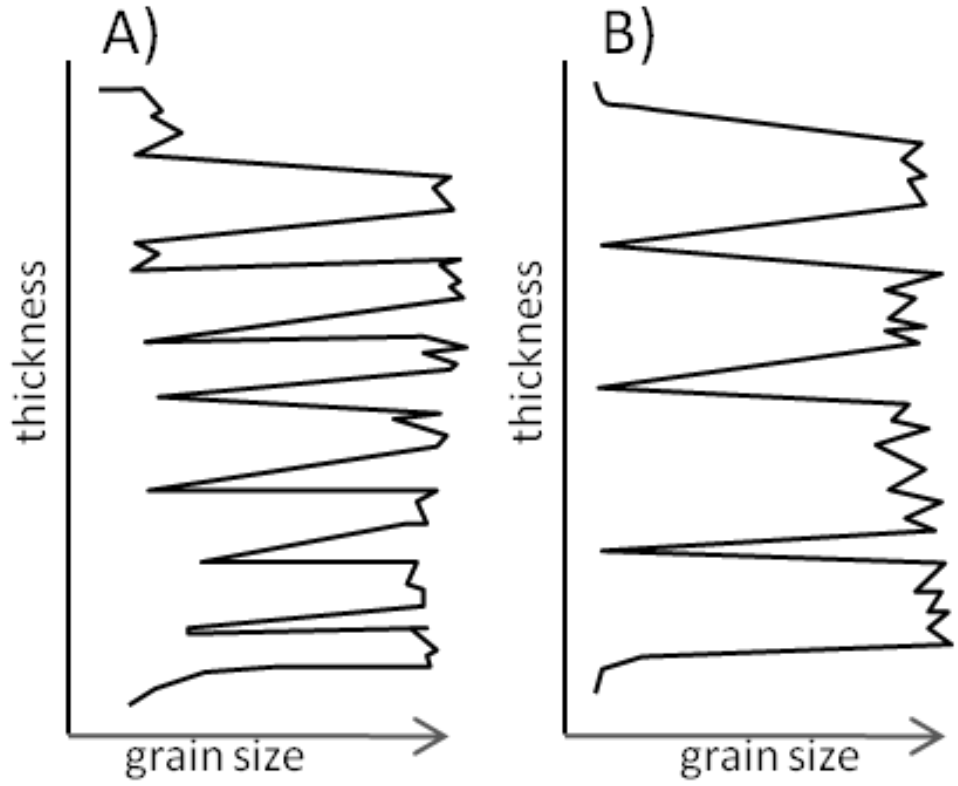

Figure 12: A) Schematic vertical section showing possible heterogeneity in a basin floor fan deposit associated with a sandy delta with a high Q_s/Q_w ratio and short, pulses of release events. B) Schematic vertical section showing possible homogeneity in a basin floor fan deposit associated with a sand delta with a low Q_s/Q_w ratio and long periods of release.

pulses of autogenic sediment delivery as would be the case from a sandy delta with similar sediment flux and water discharge characteristics: a heterogeneous deposit with thin sandy beds and thin fine grained beds. Figure 12B depicts a vertical section through a hypothetical basin floor fan with longer periods and larger magnitudes of sediment delivery from a sandy delta similar to experiment HwLs: a more homogeneous deposit with thicker sand beds and fine grained beds. This sort of interpretation can be applied to the Miocene Marnoso-arenacea Formation, northern Apennines [*Lucchi & Valmori*, 1980]. *Lucchi & Valmori* [1980] analyzed basin plain deposits that consisted of about 200 meters of turbidites that composed 80-90% of the facies present. They used eighteen measured sections to show that turbidite deposits could be correlated for long distancse and were aerially continuous. While the purpose of this study was to show that basin deposits could be correlated for wide distances, in doing so, the authors have shown distinct vertical changes in the number of beds and mean thicknesses of turbidite and sandstone beds separated by a marker (Contessa marker) documenting a change in supply conditions for the sediment source. The authors have shown lateral variations and similarities in these deposits, but the vertical variations were not analyzed except to be attributed to a change in supply. This vertical change can be interpreted as depositional signatures that result from changes in autogenic processes as supply conditions change. Before the Contessa marker (i.e. pre-Contessa), the total number of turbidite layers and sandstone beds were much lower than post-Contessa deposits (1290 pre-Contessa to 1753 post-Contessa for turbidite layers and 1008 pre-Contessa to 1250 post-Contessa for sandstone beds). Also the average thickness of turbditie layers decreases from 52 cm pre-Contessa to 48 cm post-Contessa while the average thickness of sandstone beds decreases from 32 cm to 28 cm from pre-Contessa to post-Contessa sections. The thicker, less numerous deposits of the pre-Contessa could be attributed to source discharge conditions

similar to HwLs and the thinner, more numerous deposits of the post-Contessa could be attributed to source discharge conditions similar to LwLs reflecting changes in the autogenic storage and release mechanisms of the fluvio-deltaic source system.

In stratigraphy, the alternation between channelization and sheet flow deposits can be seen experimentally [*Kim & Jerolmack*, 2008; *Sheets et al.*, 2002], and interpreted from field cases [*Goldring & Bridges*, 1972]. In an experimental study, *Sheets et al*. [2002] show sliced experimental deposits with channel-fill structures separated by lateral sheets that are not the products of channelized deposition. This is compared to deposits from Canterbury Plains, New Zealand in which channel structures are separated by lateral deposits. This succession can be derived from autogenic storage and release processes. *Kim & Jerolmack* [2008] show alternations in experimental foreset deposits that alternate between coarse and fined grained sediments due to alternations between channelized flow and sheet flow respectively. In other field examples, laterally extensive sand sheet facies and channel facies can be seen in concert with each other. *Goldring & Bridges* [1973] describe examples of channel fills that are directly above or below sand sheets. Sheet sandstones, interpreted to be associated with shallow marine open shelf environments and shoreline associations, are found either vertically above or below fluvial channel deposits. The authors interpret the vertical change from channel fills to sheet like facies as due to high tidal ranges, but the interpretation of the sheet like facies could be due to fluvial sheet flow instead of generic shelf sands. Therefore, this stratigraphic succession could be due to autogenic storage and release processes that cut and fill channels and deposit laterally extensive sheet sands from sheet flow. Because this autogenic process involves a cycle of strong channelization and incision, the development of erosional boundaries, or unconformities, becomes important. With each portion of the cycle where channelization is dominant, cutting may lead to the development of erosional boundaries.

Van Dijk et al. [2009] estimated natural autogenic incision depths due to autogenic sediment release to range between 5-10 m. Overall incision depths can be related to the buffer size which has been shown to vary with changes in sediment flux. A high discharge system, such as alluvial fans, would have significant erosion head cuts driven by autogenic processes. It is generally thought that erosional surfaces are generally attributed to some sort of change in allogenic conditions, such as base level fall. However, it is important to acknowledge that erosional surfaces and channelization can develop by purely autogenic inductions, so alternate explanations for erosional boundaries could be autogenic.

Future Work

While a great deal of progress has been made in understanding and quantifying autogenic processes from recent theoretical and experimental studies, there is still more research that needs to be done in order to link stratigraphic signatures of autogenic processes with changes in relative base level (sea level changes and/or tectonic subsidence/uplift), which we purposely eliminated in this study. The ability to recognize modifications in autogenic records due to external forcing is crucial to advance interpretation of paleo-depositional environments in preserved strata. More experiments need to be conducted under simple boundary conditions to gain first order understandings in how relative base level affects these internally generated processes in terms of the rate and magnitude of sea level rise/fall and also basin configuration (foreland basins, passive margins). Longer duration experiments that record more storage and release events, which here were constrained by the limited size of the experimental basin, would enhance current analysis in order to further understand autogenic processes.

Conclusions

Data from physical sedimentation experiments have shown fluctuations in shoreline migration rates due to fluvial autogenic storage and release processes without changes in external conditions. The present set of experiments, with a range of Q_s and Q_w, fill in missing components from previous work and provide a better understanding about how changes in sediment flux and water discharge affect autogenic timescales and also how storage and release events can be significant for modern field examples and ancient field cases. The experimental results have been shown that the relationship between Q_s, Q_w, and Q_s/Q_w ratio are quite complex in relation to the timescale of autogenic storage and release events, but there are other important correlations as summarized below:

1. The evolution of a radially growing, three-dimensional deltaic shoreline can be numerically modeled as a function of the cube root of time ($t^{1/3}$), capturing the pattern of the shoreline and shelf edge trajectory.
2. Increasing the sediment supply in a deltaic system will primarily decrease the autogenic timescale. However, the increase in sediment supply does not proportionally reduce the autogenic timescale because the increase in sediment supply yields the secondary effect on the morphology of the fluvial system by developing a relatively larger fluvial buffer to be filled during times of sediment storage.
3. Increasing the water discharge in a deltaic system will lengthen the autogenic timescale by shaping the fluvial system to be a more highly organized channel network. This highly organized pattern tends to take a longer time to develop and increases the time necessary for storage and release processes.

4. The timescale of autogenic storage and release events is negatively correlated with the Q_s/Q_w ratio between 0.015 and 0.246 in the nine experiments presented here. However, complicated interplay between the secondary effects by the Q_s/Q_w ratio and the individual values of Q_s and Q_w yields a range of autogenic timescales for a given ratio that is affected by the differential effectiveness of the Q_s and Q_w controls on the fluvial evolution under different Q_s/Q_w ratios. The secondary effects of sediment supply diminish at lower ratios while the effects of water discharge vary at lower ratios and vice versa. The range of autogenic timescales tends to increase with a smaller ratio and narrows with a larger ratio.

Appendix A: Notation

Q_s	sediment flux, cm^3s^{-1}
Q_w	water discharge, cm^3s^{-1}
S_t	topset slope, dimensionless
S_f	foreset slope, dimensionless
s	downstream shoreline position, cm.
u	downstream delta toe position, cm.
Z	absolute base level, cm.
H	upstream topset height, cm
t	time, s.
α	Constant
β	constant
p	Constant
L	characteristic basin length, cm.
h	channel depth, cm.
T_{DC}	equilibrium timescale, s.

References

Ashmore, P. (1991), Channel morphology and bed load pulses in braided, gravel-bed streams. *Geografiska Annaler. Series A, Physical Geography*, 73(1), 37-52.

Ashworth, P.J., J.L. Best, and M. Jones (2004), Relationship between sediment supply and avulsion frequency in braided rivers. *Geology(Boulder)*, 32(1), 21-24.

Berg, O.R. (1982), Seismic detection and evaluation of delta and turbidite sequences: Their application to exploration for the subtle trap. *American Association of Petroleum Geologists Bulletin*, 66(9), 1271-1288.

Bryant, M., P. Falk, and C. Paola (1995), Experimental study of avulsion frequency and rate of deposition. *Geology (Boulder)*, 23(4), 365-368.

Carvajal. C.R. and R.J. Steel (2006), Thick turbidite successions from supply-dominated shelves during sea-level highstand. *Geology*, 34(8), 665-668.

Carvajal, C. and R.J. Steel (2009), Shelf-edge architecture and bypass of sand to deep water: Influence of shelf-edge processes, sea level, and sediment supply. *Journal of Sedimentary Research*, 79, 652-672.

Castelltort, S. and J. Van Den Driessche (2003), How plausible are high-frequency sediment supply-driver cycles in the stratigraphic record? *Sedimentary Geology*, 157, 3-13.

Cazanacli, D., C. Paola, and G. Parker (2002), Experimental steep, braided flow: Application to flooding risk on fans. *Journal of Hydraulic Engineering*, 128, 322-330.

Edwards, M.B. (1981), Upper Wilcox Rosita delta system of south Texas: Growth-fault shelf-edge deltas. *American Association of Petroleum Geologists Bulletin*, 65, 54-73.

Erkens, G., R. Dambeck, K.P. Volleberg, M.T.I.J. Bouman, J.A.A. Bos, K.M. Cohen, J. Wallinga, W.Z. Hoek (2009), Fluvial terrace formation in the northern Upper Rhine Graben during the last 20,000 years as a result of allogenic controls and autogenic evolution, *Geomorphology*, 103, 476-495.

Galloway, W.E. (1989a), Genetic stratigraphic sequences in basin analysis-part I: architectures and genesis of flooding-surface bounded depositional units. *American Association of Petroleum Geologists Bulletin*, 73, 125-142.

Galloway, W.E. (1989b), Genetic stratigraphic sequences in basin analysis-part II: application to northwest Gulf of Mexico Cenozoic basin. *American Association of Petroleum Geologists Bulletin*, 73, 143-154.

Gerber, T.P., L.F. Pratson, M.A. Wolinsky, R.J. Steel, J. Mohr, J.B. Swenson, and C. Paola (2008), Clinoform progradation by turbidity currents: Modeling and Experiments. *Journal of Sedimentary Research*, 78, 220-238.

Goldring, R. and P. Bridges (1973), Sublittoral sheet sandstones. *Journal of Sedimentary Petrology*, 43(3), 736-747.

Helland-Hansen, W. and J.G. Fjelberg (1994), Conceptual basis and variability in sequence stratigraphy: a different perspective. *Sedimentary Geology*, 92, 31-52.

Helland-Hansen, W. and O.J. Martinsen (1996), Shoreline trajectories and sequences: description of variable depositional-dip scenarios. *Journal of Sedimentary Research*, 66, 670-688.

Heller, P.L., B.A. Burns, and M. Marzo (1993), Stratigraphic solution sets for determining the roles of sediment supply, subsidence, and sea level on transgressions and regressions. *Geology*, 21, 747-750.

Heller, P.L., C. Paola, I.G. Hwang, B. John, and R.J. Steel (2001), Geomorphology and sequence stratigraphy due to slow and rapid base-level changes in an experimental subsiding basin (XES 96-1). *American Association of Petroleum Geologists Bulletin*, 85, 817-838.

Hickson, T.A., B. A. Sheets, C. Paola, and M. Kelberer (2005), Experimental test of tectonic controls on three-dimensional alluvial facies architecture. *Journal of Sedimentary Research*, 75, 710-722.

Hogg. S. (1982), Sheetfloods, Sheetwash, Sheetflow, or …? *Earth-Science Reviews*, 18, 59-76.

Holbrook, J., R.W. Scott, and F.E. Oboh-Ikuenobe (2006), Base-level buffers and buttresses: A model for upstream versus downstream control on fluvial geometry and architecture within sequences. *Journal of Sedimentary Research*, 76, 162-174.

Jerolmack, D.J. and D. Mohrig (2005), Frozen dynamics of migrating bedforms. *Geology*, 33(1), 57-60.

Jerolmack, D.J. and C. Paola (2010), Shredding of environmental signals by sediment transport. *Geophysical Research Letters*, 37, 1-5.

Johannessen, E.P. and R.J. Steel (2005), Shelf-margin clinoforms an prediction of deepwater sands. *Basin Research*, 17, 521-550.

Kim, W. and D.J. Jerolmack (2008), The pulse of calm fan deltas. *The Journal of Geology*, 116, 315-330.

Kim, W. and T. Muto (2007), Autogenic response of alluvial-bedrock transition to base-level variation: Experiment and theory. *Journal of Geophysical Research-Eath Surface*, 112, F03S14.

Kim, W. and C. Paola (2007), Long-period cyclic sedimentation with constant tectonic forcing in an experimental relay ramp. *Geology*, 35(4), 331-334.

Kim, W., C. Paola, J.B. Swenson, and V.R. Voller (2006a), Shoreline response to autogenic processes of sediment storage and release in the fluvial system. *Journal of Geophysical Research-Earth Surface*, 111, F04013.

Kim, W., C. Paola, V.R. Voller, and J.B. Swenson (2006b), Experimental measurement of the relative importance of controls on shoreline migration. *Journal of Sedimentary Research*, 76(2), 270-283.

Kim, W., B.A. Sheets, and C. Paola (2010), Steering of experimental channels by lateral basin tilting. *Basin Research*, 22, 286-301.

Kolla, V. and M.A. Perlmutter (1993), Timing of turbidite sedimentation on the Mississippi Fan. *American Association of Petroleum Geologists Bulletin*, 77(7), 1129-1141.

Kostic, S., G. Parker, and J.G. Marr (2002), Role of turbidity currents in setting the foreset slope of clinoforms prograding into standing fresh water. *Journal of Sedimentary Research*, 72(3), 353-362.

Lucchi, F.R., and E. Valmori (1980), Basin-wide turbidites in a Miocene, over-supplied deep-sea plain: a geometrical analysis. *Sedimentology*, 27, 241-270.

Martin, J., C. Paola, V. Abreau, J. Neal, and B. Sheets (2009), Sequence stratigraphy of experimental strata under known conditions of differential subsidence and variable base level. *American Association of Petroleum Geologists Bulletin*, 93, 503-553.

Martin, J., B. Sheets, C. Paola, and D. Hoyal (2009), Influence of steady base-level rise on channel mobility, shoreline migration, and scaling properties of a cohesive experimental delta. *Journal of Geophysical Research*, 114, F03017.

Mohrig, D., P.L. Heller, C. Paola, and W.J. Lyons (2000), Interpreting avulsion process from ancient alluvial sequences: Guadalope-Matarranya system (northern Spain) and Wasatch Formation (western Colorado). *Geological Society of America Bulletin*, 112(12), 1787-1803.

Muto, T. (2001), Shoreline autoretreat substantiated in flume experiments. *Journal of Sedimentary Research*, 71(2), 246-254.

Muto, T. and R.J. Steel (2001), Autostepping during the transgressive growth of deltas: results from flume experiments. *Geology (Boulder)*, 29(9), 771-774.

Muto, T. and R.J. Steel (004), Autogenic response of fluvial deltas to steady sea-level fall: Implications from flume-tank experiments. *Geology*, 32(5), 401-404.

Muto, T., R.J. Steel, and J.B. Swenson (2007), Autostratigraphy: A framework norm for genetic stratigraphy. *Journal of Sedimentary Research*, 77(1), 2-12.

Muto, T. and J.B. Swenson (2006), Autogenic attainment of large-scale alluvial grade with steady sea-level fall: An analog tank-flume experiment. *Geology*, 34(3), 161-164.

Paola, C. (2000), Quantitative models of sedimentary basin filling; Millenium reviews. *Sedimentology*, 47(Suppl. 1), 121-178.

Paola, C., J. Mullins, C. Ellis, D.C. Mohrig, J.B. Swenson, G.S. Parker, T. Hickson, P.L. Heller, L. Pratson, J. Syvitski, B. Sheets, and N. Strong (2001), Experimental Stratigraphy. *GSA Today*, 4-9.

Paola, C., K. Straub, D. Mohrig, and L. Reinhardt (2009), The "unreasonable effectiveness" of stratigraphic and geomorphic experiments. *Earth-Science Reviews*, 97, 1-43.

Parker, G., C. Paola, K. Whipple, and D. Mohrig (1998), Alluvial fans formed by channelized fluvial and sheet flow. I: Theory. *Journal of Hydraulic Engineering*, 124, 985-995.

Petter, A.L. and T. Muto (2008), Sustained alluvial aggradation and autogenic detachment of the alluvial river from the shoreline in response to steady fall of relative sea level. *Journal of Sedimentary Research*, 78, 98-111.

Porebski, S.J. and R.J. Steel (2003), Shelf-margin deltas: their stratigraphic significance and relation to deepwater sands. *Earth-Science Reviews*, 62, 238-326.

Posamentier, H.W. and P.R. Vail (1988), Eustatic controls on clastic deposition II – sequence and systems track models, in Sea-Level Changes: An Integrated Approach, *SEPM Special Publication*, 42, 125-154.

Posamentier, H.W., M.T. Jervey, and P.R. Vail (1988), Eustatic controls on clastic deposition I – conceptual framework, in Sea-Level Changes: An Integrated Approach, *SEPM Special Publication*, 42, 109-124.

Postma, G., M.G. Kleinhans, T.H. Meijer, and J.T. Eggenjuisen (2008), Sediment transport in analogue flume models compared with real-world sedimentary systems: a new look at scaling evolution of sedimentary systems in a flume. *Sedimentology*, 55, 1541-1557.

Reitz, M.D., D.J. Jerolmack, and J.B. Swenson (2010), Flooding and flow path selection on alluvial fans and deltas. *Geophysical Research Letters*, 37, L06401.

Sheets, B.A., T.A. Hickson, and C. Paola (2002), Assembling the stratigraphic record: depositional patterns and time-scales in an experimental alluvial basin. *Basin Research*, 14, 287-301.

Swenson, J.B., V.R. Voller, C. Paola, G. Parker, J.G. Marr (2000), Fluvio-deltaic sedimentation: A generalized Stefan problem. *Euro. Jnl of Applied Mathematics*, 11, 433-452.

Vail, P.R., R.M. Mitchum, and S. Thompson (1977), Seismic stratigraphy and global changes of sea level, III: Relative changes of sea level from coastal onlap in Seismic Stratigraphy; Applications to Hydrocarbon Exploration. *American Association of Petroleum Geologists Memoir*, 26, 63-97.

Van Dijk, M., G. Postma, and M.G. Kleinhans (2009), Autocyclic behavior of fan deltas: an analogue experimental study. *Sedimentology*, 56, 1569-1589.

Van Wagoner, J.C., H.W. Posamentier, R.M. Mitchum, P.R. Vail, J.F. Sarg, T.S. Loutit, and J. Hardenbol (1988), An overview of the fundamentals of sequence stratigraphy and key definitions, in Sea Level Changes: An Integrated Approach. *SEPM Special Publication*, 42, 39-45.

Watts, A.B. (1982), Tectonic subsidence, flexure and global changes of sea level. *Nature*, 297, 469-474.

Whipple, K.X., G. Parker, C. Paola, and D. Mohrig (1998), Channel dynamics, sediment transport, and the slope of alluvial fans: Experimental study. *Journal of Geology*, 106, 677-693.